Cell PRESS
Cancer Cell
Article

EphA3 Maintains Tumorigenicity and Is a Therapeutic Target in Glioblastoma Multiforme

Bryan W. Day,[1,*] Brett W. Stringer,[1] Fares Al-Ejeh,[2] Michael J. Ting,[1] John Wilson,[4] Kathleen S. Ensbey,[1] Paul R. Jamieson,[1] Zara C. Bruce,[1] Yi Chieh Lim,[1] Carolin Offenhäuser,[1] Sara Charmsaz,[1] Leanne T. Cooper,[1] Jennifer K. Ellacott,[1] Angus Harding,[4] Lucie Leveque,[3] Po Inglis,[1,5] Suzanne Allan,[1,5] David G. Walker,[6] Martin Lackmann,[7] Geoffrey Osborne,[4] Kum Kum Khanna,[2] Brent A. Reynolds,[8] Jason D. Lickliter,[1,9] and Andrew W. Boyd[1,4,10]
[1]Brain Cancer Research Unit and Leukaemia Foundation Research Unit
[2]Signal Transduction Laboratory
[3]Antigen Presentation and Immunoregulation Laboratory
Queensland Institute of Medical Research, Brisbane 4006, Australia
[4]Queensland Brain Institute, University of Queensland, Brisbane 4067, Australia
[5]Cancer Services, Royal Brisbane and Women's Hospital, Brisbane 4024, Australia
[6]BrizBrain & Spine Research Foundation, Auchenflower, Brisbane 4066, Australia
[7]Department of Biochemistry and Molecular Biology, Monash University, Melbourne 3800, Australia
[8]McKnight Brain Institute, University of Florida, Gainesville, FL 32611, USA
[9]Centre for Cancer Research, Monash Institute of Medical Research, Melbourne 3168, Australia
[10]Department of Medicine, University of Queensland, Herston, Brisbane 4006, Australia
*Correspondence: bryan.day@qimr.edu.au
http://dx.doi.org/10.1016/j.ccr.2013.01.007

SUMMARY

Significant endeavor has been applied to identify functional therapeutic targets in glioblastoma (GBM) to halt the growth of this aggressive cancer. We show that the receptor tyrosine kinase EphA3 is frequently overexpressed in GBM and, in particular, in the most aggressive mesenchymal subtype. Importantly, EphA3 is highly expressed on the tumor-initiating cell population in glioma and appears critically involved in maintaining tumor cells in a less differentiated state by modulating mitogen-activated protein kinase signaling. EphA3 knockdown or depletion of EphA3-positive tumor cells reduced tumorigenic potential to a degree comparable to treatment with a therapeutic radiolabelled EphA3-specific monoclonal antibody. These results identify EphA3 as a functional, targetable receptor in GBM.

INTRODUCTION

Glioblastoma (GBM) is the most common primary brain cancer. Standard treatment involves surgical resection, followed by radiation and temozolomide chemotherapy (Behin et al., 2003). Therapy is rarely curative due to the infiltrative nature of these tumors and their resistance to radiation and chemotherapy. Median survival is <15 months and median progression-free survival is <7 months (Stupp et al., 2005). This dismal situation motivates a search for new therapies, in particular those that target tumor-propagating cells. Gene expression profiling, together with DNA mutation data, has identified four GBM subtypes (proneural, neural, classical, and mesenchymal) (Carro et al., 2010; Verhaak et al., 2010). There is also accumulating evidence that at least some GBMs arise from developmentally arrested neural progenitor or stem cells (Pardal et al., 2003; Reya et al., 2001; Singh et al., 2004), although this may not be universally true (Visvader, 2011). Despite this controversy, cells with dedifferentiated properties are thought to be responsible for tumor recurrence following treatment (Dick, 2008), and their intrinsic resistance to both chemotherapy and radiation requires new strategies to eradicate them (Bao et al., 2006).

Eph receptors are the largest family of receptor tyrosine kinases and have vital functions, including cell adhesion, migration, and axon guidance, during development and homeostasis (Flanagan and Vanderhaeghen, 1998; Holder and Klein, 1999;

Significance

Although debate still surrounds the cancer stem cell hypothesis in solid tumors, such as GBM, there is agreement that cells in a less differentiated, tumorigenic state exist within these highly heterogeneous tumors. These cells are thought to be responsible for tumor recurrence following treatment. Here, we demonstrate that in EphA3-expressing GBM, EphA3 has a functional role in maintaining less differentiated, tumor-initiating cells by modulation of mitogen-activated protein kinase signaling. EphA3 is lowly expressed in adult tissues and therefore represents a relatively tumor-specific therapeutic target in GBM.

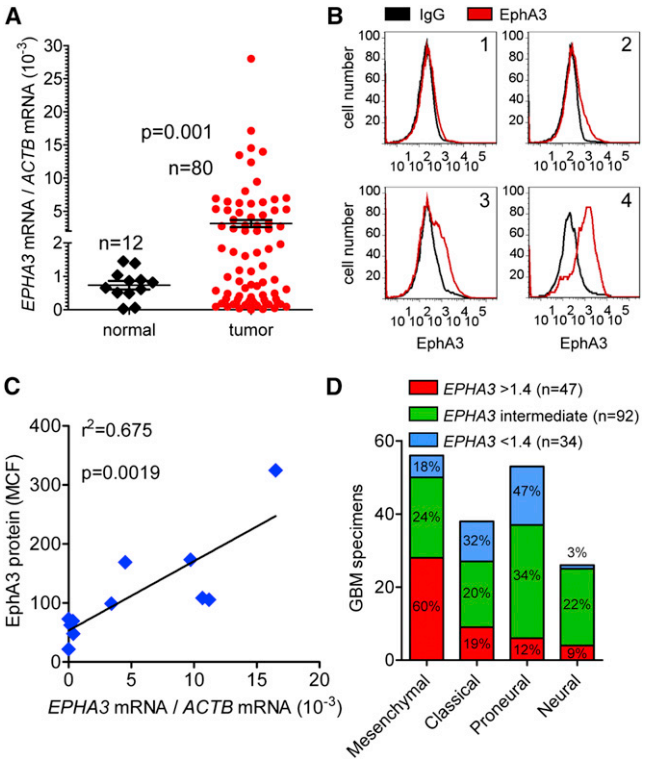

Figure 1. EphA3 Is Expressed Highly in Glioma and Is Overrepresented on Mesenchymal Tumors

(A) *EPHA3* overexpression was tested by qPCR in glioma clinical specimens (n = 80) compared to normal brain tissue (n = 12; p = 0.001; unpaired t test with Welsh's correction). *EPHA3* mRNA levels were negligible in normal brain while 40% of clinical specimens (32/80) expressed detectable levels of *EPHA3* mRNA (more than two copies per 1,000 β-actin; further defined in Figure S1). Table S1 lists the specimens tested.

(B) Flow cytometric analysis of EphA3 protein expression in dissociated GBM clinical specimens.

(C) Linear regression analysis of *EPHA3* mRNA (qPCR) and EphA3 protein (mean channel fluorescence) levels in serum-free cultures (n = 11) shows a positive correlation (r^2 = 0.675, p = 0.0019). See also Figure S1.

(D) *EPHA3* microarray expression data were compared to GBM subtype classification (mesenchymal, classical, proneural, neural) in GBM specimens from the TCGA database (n = 173). Samples expressing *EPHA3* >1.4-fold (n = 47) showed an overrepresentation of mesenchymal tumors (60%) and an underrepresentation of neural tumors (9%). The difference between each group was significant (p = 0.001) as assessed by multivariate analysis. See also Figures S1A–S1F.

Mann et al., 2002; Wilkinson, 2000). Eph receptors and ephrin ligands tend to be most highly expressed during development, and evidence suggests a role in regulation of stem cell differentiation and cell fate determination (Aoki et al., 2004; Conover et al., 2000; Holmberg et al., 2006; Lickliter et al., 1996; Wang et al., 2004). Ephrins and Eph receptors have been found to be aberrantly expressed in many cancers, including GBM (Pasquale, 2010). Family members implicated in gene deregulation and function in GBM include EphA2, EphA7, EphB2, and ephrin-A5 (Li et al., 2009; Nakada et al., 2004; Wang et al., 2008; Wykosky et al., 2005).

EphA3 is expressed in embryonic tissues including the brain, spinal cord, axial muscles, lungs, kidneys, and heart (Kilpatrick et al., 1996) and appears to play a critical role in epithelial-to-mesenchymal transition (EMT) (Stephen et al., 2007). EphA3 mutations have been identified that suggest a tumor-suppressor role in some cancers (Davies et al., 2005). Conversely, overexpression of EphA3 has been observed in some cancers, including leukemia, lymphoma, lung cancers, melanomas, and gastric carcinoma (Boyd et al., 1992; Chiari et al., 2000; Dottori et al., 1999; Lawrenson et al., 2002; Wicks et al., 1992; Xi et al., 2012). EphA3 somatic mutations, which map to highly conserved regions of the gene, have been identified in GBM (Balakrishnan et al., 2007; Lisabeth et al., 2012).

Given the expression of EphA3 in many human cancers and its role in EMT, we explored the expression and function of EphA3 in GBM and, in particular, the mesenchymal subtype, which has a more aggressive and less differentiated phenotype with a poorer prognosis (Phillips et al., 2006).

RESULTS

EphA3 Is Highly Expressed in Glioma and Is Overrepresented on Mesenchymal GBM

To investigate EphA3 expression in brain cancer, we assessed messenger RNA (mRNA) and protein levels in a series of clinical glioma specimens and specimen-derived early passage cell lines. A bank of 80 human glioma clinical specimens was collected of which 74% were GBM (WHO grade IV) (Table S1 available online). Quantitative PCR (qPCR) was performed on these tumors and 12 normal human brain specimens (Figure 1A). *EPHA3* mRNA levels were low in normal brain whereas 40% of clinical specimens (32/80) expressed significantly ($p < 0.01$) higher levels of *EPHA3* mRNA. EphA3 protein expression was assessed using flow cytometry of dissociated GBM tumor samples; representative expression profiles are shown in Figure 1B. In some cases essentially all cells were positive, whereas in others only a subset showed significant expression.

To further explore EphA3 expression, we analyzed a panel of early passage (less than five passages) cell lines from primary GBM specimens. Lines were grown in serum-free medium on a laminin substratum, because these conditions are reported to maintain the phenotype and genotype of the original tumor and enrich for tumor-initiating cells (Pollard et al., 2009). qPCR and flow cytometry were used to analyze EphA3 expression in these cultures (Figures S1A and S1B). Results showed that a greater proportion of cultures expressed *EPHA3* (60%, n = 15) compared to clinical specimens (40%, n = 80). Flow cytometry also revealed a greater than expected level of EphA3 expression when compared to the original tissue specimens (data not shown).

To determine the correlation between mRNA and protein expression, we analyzed primary serum-free cultures (n = 11) to compare mRNA (qPCR) and protein (mean channel fluorescence) levels (Figure 1C). Linear regression analysis showed a strong correlation (r^2 = 0.675 p = 0.0019) between mRNA and protein expression. EphA3 protein was detectable by flow cytometry when GBM lines expressed mRNA levels of two or more copies per 1,000 β-actin (Figure S1C). Additional analysis of ephrin expression by qPCR was performed in six primary serum-free cultures (Figure S1D). All samples had relatively low expression and, in particular, of the high-affinity *EPHA3* ligand *EPHRIN A5*.

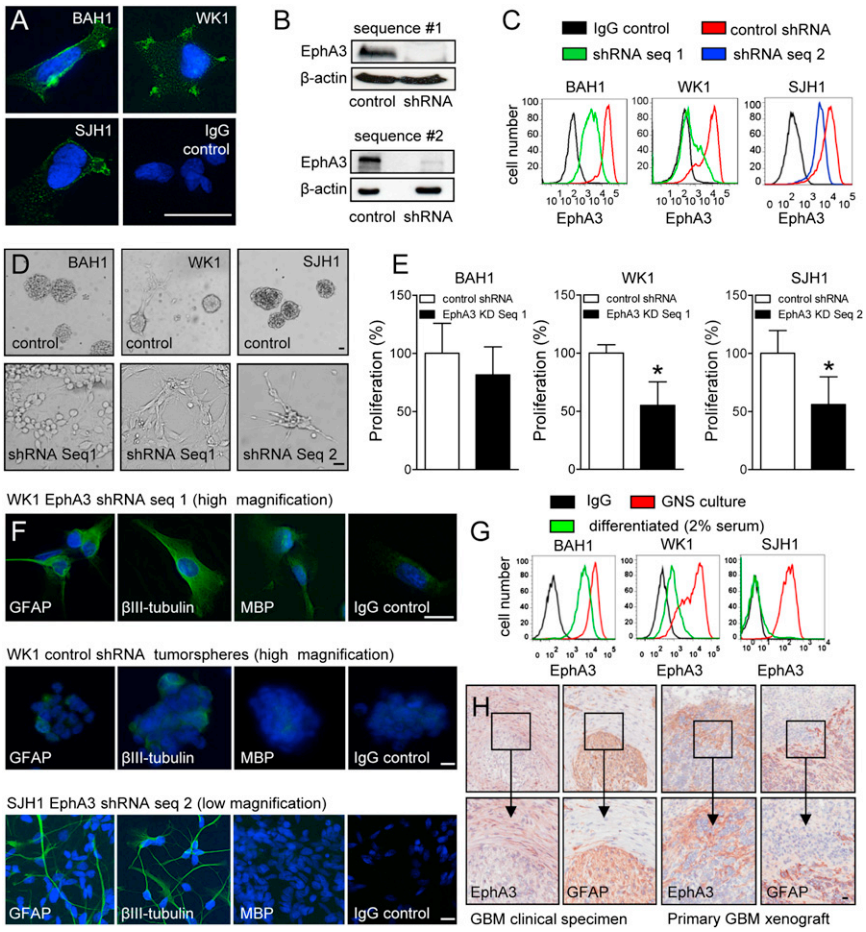

Figure 2. EphA3 Neutralization Prevents Tumorsphere Formation and Induces Neuronal and Glial Cell Differentiation

(A) Immunofluorescence staining of EphA3 in three early passage primary GBM cultures (BAH1, WK1, and SJH1) reveals EphA3 is abundantly expressed and localized at the cell membrane.

(B) EphA3 protein level was downregulated using two *EPHA3* shRNA sequences.

(C) EphA3 downregulation in primary GBM cultures was quantified using flow cytometric analysis. The most effective KD in BAH1 and WK1 cells was achieved using shRNA sequence 1, whereas shRNA sequence 2 was proven more effective in SJH1 cells. Staining levels were compared to control shRNA.

(D and E) Downregulation of EphA3 induced a partial loss of tumorsphere formation and reduced proliferation in all three primary GBM lines following cell passage (*$p < 0.05$, +SD, $n = 3$).

(F) EphA3 downregulation coincided with positive staining of neuronal (βIII-tubulin) and glial (GFAP) differentiation markers, which was low in control tumorspheres (data shown for WK1 and SJH1).

(G) EphA3 levels were assessed by flow cytometry following differentiation of BAH1, WK1, and SJH1 cells. Differentiation was induced by removal of growth factors and addition of 2% serum. A reduction in EphA3 was observed in each line when compared to cells cultured under dedifferentiating serum-free conditions.

(H) Immunohistochemical staining of sequential sections of a GBM clinical specimen and a BAH1 GBM xenografted tumor shows highly discrete staining between EphA3 and the glial marker GFAP.

Scale bar represents 20 μM. See also Figures S2A–S2F.

To investigate if *EPHA3* expression correlated with glioma subtypes, we analyzed a data set of GBM specimens from The Cancer Genome Atlas Project (TCGA) ($n = 173$), which had been assigned GBM subtypes defined by a previous study (Verhaak et al., 2010). Samples expressing elevated *EPHA3* (>1.4-fold; $n = 47$) showed an overrepresentation of mesenchymal tumors (60%) and an underrepresentation of neural tumors (9%), which was significant by multivariate analysis ($p = 0.0001$) (Figure 1D). Furthermore, analysis of *EPHA3* alterations, the majority being RNA upregulation, using the TCGA database revealed that altered *EPHA3* led to decreased survival in patients with mesenchymal subtype GBM ($n = 56$, $p = 0.017$; Figure S1E). Alternatively, using the Rembrandt database, *EPHA3* expression in all gliomas ($n = 454$) showed a significant correlation with survival (Figure S1F). Analysis revealed a 2-fold decrease in *EPHA3* expression ($n = 160$) correlated with increased survival ($p = 0.002$), whereas a 2-fold increase in *EPHA3* expression ($n = 34$) correlated with decreased survival ($p = 0.02$).

Loss of EphA3 Prevents Tumorsphere Formation and Induces Neuronal and Glial Cell Differentiation

Growth under neurosphere culture conditions selects against survival of terminally differentiated cells, whereas less differentiated cells respond to growth factors to form "neurospheres" (Reynolds and Weiss, 1992). Under these conditions, a subset of GBM cells grow as "tumorspheres" and exhibit self-renewal and retain the capacity to differentiate (Galli et al., 2004). Consequently, to further explore EphA3 function in GBM, we generated three primary GBM cultures (BAH1, WK1, and SJH1), which were all shown to form orthotopic tumors in immune-compromised animals; we also used the established GBM cell line U251 grown as tumorspheres. The subtype of these primary lines was determined using the microarray method outlined by Verhaak et al. (2010). BAH1 and SJH1 were derived from GBMs of the neural subtype while WK1 was established from a mesenchymal GBM. Immunofluorescence staining for EphA3 showed strong membranous expression in all of the lines (Figure 2A).

We first investigated the effect of EphA3 knockdown (KD) on tumorsphere growth using two different *EPHA3* small hairpin RNA (shRNA) sequences, both of which resulted in >90% KD of EphA3 expression (Figures 2B, 2C, S2A, and S2B). In all four cell lines, following several passages the sphere-forming capability of the KD cells was reduced and was accompanied by increased cell spreading, adherence, and morphological changes (Figures 2D and S2C). Adherent cells in all three EphA3 KD primary lines grew slowly under tumorsphere culture conditions and died following subsequent cell passage. This

phenomenon was not observed in U251 cells, which grew slowly but remained viable (Figure S2D). In contrast, when EphA3 KD primary cells were grown under serum-free conditions on laminin, all three primary cultures were viable but proliferated slowly (Figure 2E). To determine whether the morphological changes following KD were the result of differentiation, cultures were stained with lineage-specific markers (Figures 2F and S2E). Positive staining for astrocytic (glial fibrillary acidic protein [GFAP]) and neuronal (βIII-tubulin) markers, but minimal staining with the oligodendrocytic (myelin basic protein) lineage marker, was observed. Control tumorspheres showed minimal staining for differentiation markers (Figure S2F). We also established a tetracycline-inducible EphA3 KD system in U251 cells (Figures S2B–S2E). Whereas EphA3-positive U251 cells formed tumorspheres in the absence of tetracycline, tumorsphere formation and proliferation was greatly reduced following tetracycline-induced EphA3 KD and was accompanied by expression of differentiation markers. Following removal of tetracycline, EphA3 was re-expressed and tumorsphere formation was restored. As a specificity control for EphA3 KD, we performed a rescue experiment by re-expressing EphA3 with a mutated shRNA binding site in U251 constitutive EphA3 KD cells (Figures S2C and S2D). Following re-expression of shRNA-resistant EphA3, both proliferation and tumorsphere-forming capacity were restored.

We further compared EphA3 expression in the primary lines following growth factor withdrawal and addition of 2% fetal bovine serum (FBS), conditions that allow differentiation to occur (Figure 2G). In each case EphA3 levels decreased in serum-containing medium, providing further evidence that EphA3 is downregulated during GBM cell differentiation. When recultured in serum-free medium, EphA3 levels increased to preserum culture levels with a parallel decrease in differentiated cells (data not shown). To demonstrate that EphA3 was expressed on less differentiated cells, we assessed the expression of EphA3 compared to the expression of GFAP, a marker of astrocytes, in both patient specimens and GBM tumor xenografts. Immunohistochemistry (IHC) results are shown for sequential tissue sections from a GBM patient specimen and GBM xenograft using BAH1 cells (Figures 2H and S2G). These show a specific and discrete pattern of staining for EphA3 and GFAP, implying that EphA3 expression is high on less differentiated tumor cells and reduced on the differentiated population.

EphA3 Is Coexpressed with Markers of Undifferentiated Cells in GBM

Of the markers of less differentiated, highly proliferative cells in GBM that have been reported in the literature, among the most convincing have been CD133, integrin α6, and CD15 (Lathia et al., 2010; Singh et al., 2004; Son et al., 2009). To investigate if EphA3 is coexpressed with these markers, we examined nine acutely dissociated GBM specimens using multiparameter flow cytometry, using the epidermal growth factor (EGF) receptor as a positive control (Figure 3A). Specimens did not show distinct subpopulations, but EphA3 appeared to be commonly coexpressed with integrin α6 but not CD133 (complete analysis and controls shown in Figure S3A). Association with these markers was further confirmed in the primary lines using both Amnis expression analysis (Figure 3B) and flow cytometry (Figure 3C) showing that EphA3 is most often coexpressed with integrin α6 and CD133 but not with CD15 (for complete flow cytometry analysis and controls see Figure S3B). Given that primary serum-free cultures grown on laminin are reported to enrich for the dedifferentiated, highly proliferative cells known to express such markers as CD133, integrin α6, and CD15, we assessed the expression of EphA3 using three primary GBM tissue specimens and the paired primary serum-free culture. Results show that EphA3 expression was increased under these culture conditions (Figure 3D). Despite two tissue specimens expressing low levels of EphA3, all samples showed a significant increase in EphA3 expression following culture for 3 weeks. We also assessed the expression by qPCR of neural and other progenitor cell markers in WK1 cells transfected with control shRNA versus *EPHA3* shRNA (Figure 3E). Results show a reduced expression of all these markers following EphA3 KD. Next, we sorted each primary culture into high and low EphA3 fractions and assessed the expression of progenitor cell markers, proliferation, and sphere-forming potential (Figures 3E and S3C). In each case, expression of at least one marker was elevated in the EphA3-high population; in the case of the mesenchymal line WK1, all markers were elevated in the EphA3-high fraction (Figure 3E). Moreover, in all lines tested, the EphA3-positive population showed a significantly ($p < 0.05$) higher capacity to form tumorspheres and to proliferate at a higher rate. Furthermore, IHC and immunofluorescence staining for CD31 and EphA3 in the same GBM xenograft section revealed that EphA3 was predominantly localized around the tumor vasculature (Figures 3F and S2G), a reported niche for GBM stem/progenitor cells (Calabrese et al., 2007). Thus, we have presented several lines of evidence that EphA3 is coexpressed with known markers of undifferentiated cells in both clinical specimens and primary cultures. This is in keeping with the finding that EphA3 is most commonly elevated in mesenchymal GBM, which are characterized by the presence of progenitor cell markers and lack of neural differentiation markers. Furthermore, EphA3 appears to be most commonly coexpressed with integrin α6, a GBM progenitor cell marker known to be expressed in the vascular bed of GBM tumors (Lathia et al., 2010).

EphA3 Limits MAPK Pathway Activation

Previous studies have shown that EphA receptor activation can lead to increased differentiation of neural precursor cells through positive regulation of the extracellular signal-regulated kinase (ERK) mitogen-activated protein kinase (MAPK) pathway (Aoki et al., 2004). We examined ERK1/2 phosphorylation in both WK1 and U251 cells and found that the ERK/MAPK pathway was more highly activated in EphA3 KD cells compared to control (Figures 4A and S4A). In contrast, the phosphatidylinositide 3-kinases/protein kinase B and Janus-activated kinase/signal transducer and activator of transcription pathways showed no change following EphA3 KD (data not shown). Moreover, when cells had been cultured without EGF, activation of the MAPK pathway using either receptor tyrosine kinase (RTK)-dependent (EGF) or RTK-independent (PMA [phorbol-12-myristate-13-acetate]) stimulation resulted in prolonged and elevated MAPK pathway activation when EphA3 was downregulated (Figures 4B and S4B). This suggested that the differentiation observed when EphA3 was neutralized could be due to

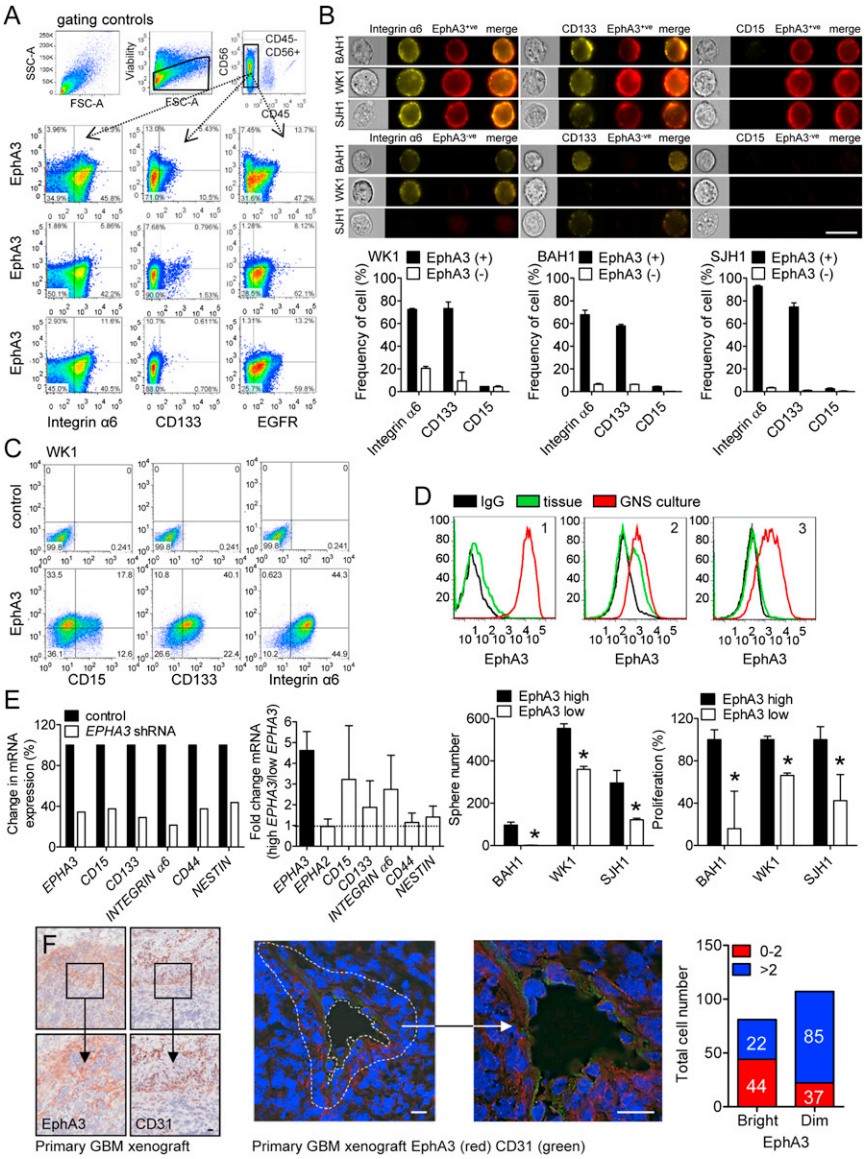

Figure 3. EphA3 Is Coexpressed with Markers of Undifferentiated Cells in GBM

(A) EphA3 coexpression with the markers integrin α6 and CD133 was assessed in GBM clinical specimens (n = 9); EGFR was used as a positive control. EphA3 was coexpressed with integrin α6, while distinct subpopulations of EphA3- and CD133-positive cells were observed in some of the samples. See Figure S3 for complete analysis and controls of nine specimens.

(B) Amnis expression analysis was performed on three primary GBM cultures for EphA3 and the markers integrinα6, CD133, and CD15; representative individual and merged fluorescent images are shown. Percentage of cells coexpressing EphA3 and the marker of interest is quantitated for each primary line (+SD, n = 3).

(C) EphA3 coexpression with the markers CD15, CD133 and integrin α6 was assessed by flow cytometry in three primary serum-free lines. Data are shown for WK1. See Figure S3 for analysis of BAH1 and SJH1.

(D) Flow cytometric analysis of paired GBM tumor tissue and serum-free culture showing expression of EphA3 is elevated under serum-free conditions compared to the original patient specimen.

(E) Stem cell-like marker expression was assessed in control shRNA versus *EPHA3* shRNA seq 1 WK1 cells. WK1 EphA3 KD cells showed a decrease in all markers tested. Expression shown as the percentage reduction in mRNA levels. Primary serum-free cultures (BAH1, WK1, and SJH1) were sorted into low and high EphA3 populations and qPCR undertaken to determine expression of undifferentiated markers, with expression shown as copy number per 1,000 β-actin. See Figure S3 for all primary lines tested. Sphere-forming potential and proliferation were also found to be significantly reduced in the EphA3-low compared to EphA3-high cells for each of the three primary lines (*$p < 0.05$, +SD; n = 3).

(F) Immunohistochemical and immunofluorescent staining of BAH1 GBM xenografted tumor shows coexpression of EphA3 and the endothelial cell marker CD31. EphA3 (red) bright cells are primarily found in close proximity to the tumor vasculature (CD31+, green). Number of bright EphA3$^+$ versus dim EphA3$^+$ cells was quantitated in a localization-dependent fashion; cells in close proximity to the CD31$^+$ cells (within two layers of cells; white dashed lines indicated boundaries) were compared to cells outside this region. Scale bar represents 20 μM. See also Figures S3A–S3D.

constitutively elevated ERK/MAPK activation. Furthermore, re-expression of EphA3 in U251 KD cells returned tumorsphere formation in parallel with a loss of constitutively activated ERK1/2 (Figure S4A). This suggested that EphA3 may be limiting MAPK signaling and thereby restricting differentiation. To further assess if ERK phosphorylation was indeed driving differentiation, we overexpressed wild-type and constitutively active mitogen-activated protein kinase kinases 1 and 2 (MEK1/2) in U251 wild-type tumorsphere cells and also downregulated ERK1/2 using small interfering RNA (siRNA) in EphA3 KD U251 tumorspheres (Figures S4C and S4D). MEK1/2 overexpression led to constitutively active ERK1/2, resulted in a loss of tumorsphere formation, and induced morphological changes indicative of differentiation and reduced cell growth. This phenomenon was reversed in EphA3 KD cells when ERK1/2 levels were reduced by siRNA-mediated KD, restoring tumorsphere formation. Another Eph receptor, EphA2, has been shown to be frequently overexpressed in GBM (Wykosky et al., 2005). We found that EphA2 was coexpressed with EphA3 on many GBM patient samples (Table S1). Immunofluorescence staining of EphA2 and EphA3 in primary lines showed significant overlapping expression patterns (Figure S4F). Some degree of association of these proteins was demonstrated by immunoprecipitation of both EphA2 and EphA3 in U251 tumorspheres and primary serum-free cultures. Given the coexpression of the two receptors, we examined the effect of *EPHA2* shRNA-mediated KD in U251 tumorspheres. Results confirmed that, similar to EphA3 attenuation, EphA2 KD prevented tumorsphere formation, reduced proliferation (33%, $p < 0.05$), and resulted in sustained ERK activation following EGF stimulation (Figure S4G).

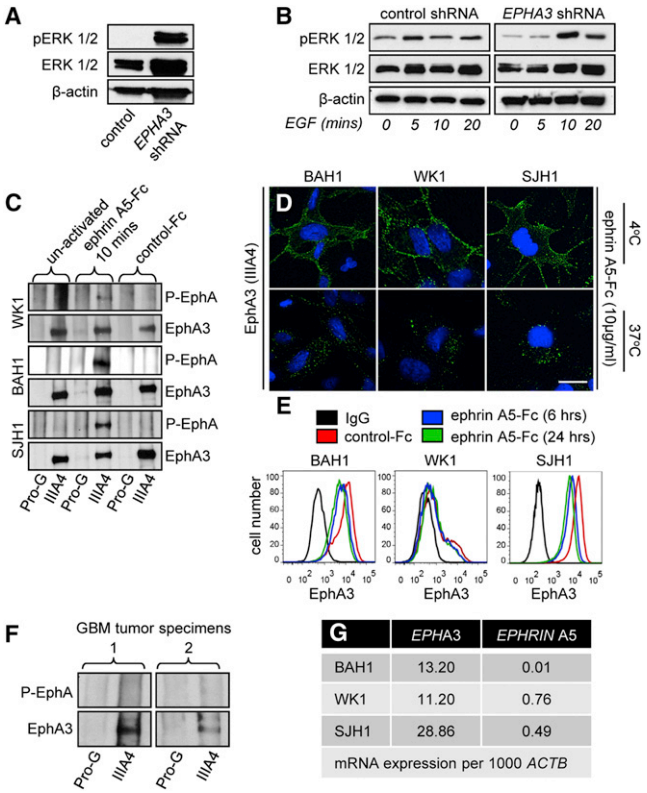

G	*EPHA3*	*EPHRIN* A5
BAH1	13.20	0.01
WK1	11.20	0.76
SJH1	28.86	0.49
mRNA expression per 1000 *ACTB*		

Figure 4. EphA3 Limits MAPK Pathway Activation and Exhibits Low Basal Receptor Activation In Vitro and In Vivo

(A) EphA3 KD in WK1 tumorspheres induces constitutive ERK1/2 activation.

(B) EphA3 KD in WK1 tumorspheres induces elevated ERK1/2 activation following treatment with EGF (30 ng/ml).

(C) Immunoprecipitation of EphA3 following treatment of BAH1, WK1, and SJH1 with soluble clustered ephrin-A5-Fc (1 μg/ml) for 10 min revealed rapid receptor activation. No activation was detected in the unstimulated primary cultures.

(D) Immunofluorescent staining of EphA3 in BAH1, WK1, and SJH1 cells showed rapid internalization of EphA3/ephrin-A5 receptor and ligand complexes following activation with ephrin-A5-Fc (10 μg/ml) for 20 min at 37°C. EphA3 remained on the cell surface if activation was delayed by maintaining the cells at 4°C. Following ephrin-A5-Fc treatment, pronounced cell spreading and adhesion were observed.

(E) Flow cytometric analysis revealed a mild reduction of EphA3 on the cell surface following treatment with ephrin-A5-Fc (10 μg/ml) for 6 and 24 hr in BAH1 WK1 and SJH1 cells; expression is compared to control CD48-Fc (24 hr).

(F) Immunoprecipitation of EphA3 in two GBM tissue specimens reveals total EphA3 was present while no receptor activation was detected.

(G) qPCR expression analysis of *EPHA3* and *EPHRIN* A5 in BAH1, WK1, and SJH1 shows elevated receptor expression compared to low ligand. Scale bar represents 20 μM. See also Figures S4A–S4G.

Aoki et al. (2004) showed that EphA3 activation could drive neural cell differentiation through increased MAPK pathway activation, whereas our data showed that EphA3 maintains an undifferentiated, self-renewing tumor population through a mechanism that limits MAPK signaling. We investigated the activation status of EphA3 in GBM cells with or without stimulation with the high-affinity ligand ephrin A5. The three primary lines tested showed low levels of kinase activity in unstimulated cultures, but the kinase was readily activated in response to stimulation with clustered ephrin A5-Fc in all lines (Figure 4C). Furthermore, EphA3 activation also led to an increase in cell spreading and rapid internalization of receptor complexes (Figure 4D), and consequently a reduction in cell-surface EphA3 expression (Figure 4E). To determine if the low kinase activity in vitro reflected the activation status in vivo, we tested its activation state in GBM patient specimens. Although EphA3 was expressed in patient samples, we could not detect kinase activity (Figure 4F). qPCR expression analysis revealed that *EPHRIN A5* expression is low in all lines (Figure 4G), which is in keeping with the expression analysis in a larger group of primary lines tested (Figure S1). Receptor activation in U251 resulted in a reduction in proliferation when high concentrations of ephrin were used (Figure S4). Because the ephrin is cleaved during internalization, we assume the high concentration is needed to maintain continued internalization of Eph receptor. Ephrin A5-Fc may also activate EphA2. Therefore, to exclude an EphA2-mediated effect, we treated U251 cells with ephrin A5-Fc following EphA2 downregulation using shRNA (Figure S4H). The EphA2 KD cells showed an ephrin A5-Fc-stimulated reduction in proliferation similar to control cells. We also specifically activated EphA3 using the EphA3 monoclonal antibody (mAb) IIIA4, which, like ephrin, results in rapid internalization (Figure 4SH) (Vearing et al., 2005). An EphA3-specific reduction in proliferation was observed in U251 cells when stimulated with IIIA4, while an EphA3-negative primary GBM line (L1-NS) was unaffected. These data suggest that although EphA3 is present and functional in GBM, it is most likely functioning in a kinase-independent fashion to decrease MAPK signaling.

EphA3 Neutralization Attenuates Tumor Formation

Because EphA3 KD induced differentiation and reduced proliferation, we asked if tumorigenesis was affected. The U251 *EPHA3* shRNA sequence 1 versus control shRNA cells were injected subcutaneously into nonobese diabetic severe combined immunodeficiency (NOD/SCID) animals (Figure S5A). There was a dramatic reduction in tumor formation in the EphA3 KD group when compared with controls. Control tumors reached the 1 cm diameter endpoint at an average of 68 days. In contrast, all EphA3 KD animals survived beyond 100 days without tumor formation. The experiment was terminated at day 140, and at autopsy only one animal was found to have a small lesion. qPCR and IHC of EphA3 showed high expression in control tumors whereas low or negligible expression was detected in the single KD tumor. This small tumor also showed high expression of GFAP and βIII-tubulin mRNA and GFAP and caspase-3 protein compared to the controls (Figures S5B and S5C).

Given the unique microenvironment in the brain, we also examined the antitumor potential of both EphA3 neutralization and depletion of EphA3 on the formation of intracranial xenografts. Initially, U251 EphA3 KD versus control shRNA cells were injected into the right hemisphere of NOD/SCID animals. As in the subcutaneous xenograft model, a failure of tumor formation was observed in mice injected with the KD cells (Figure 5SD), whereas control animals formed large, well-vascularized, invasive tumors at an average of 78 days after implantation. All EphA3 KD animals were free of tumor at autopsy on day 145 postimplantation. To exclude off-target shRNA effects, mutant EphA3 rescue cells were also analyzed. Control shRNA and

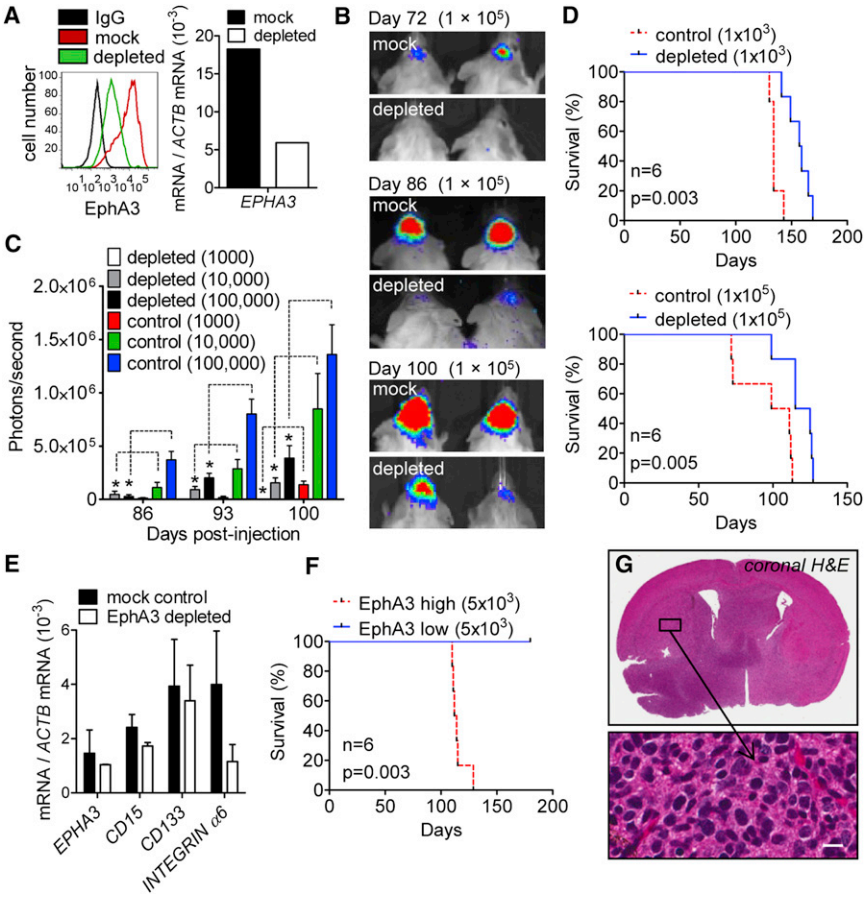

Figure 5. EphA3 Ablation Induces Differentiation and Delays GBM Tumor Progression In Vivo

(A) Flow cytometric and qPCR expression analysis of EphA3 in WK1 serum-free cells following depletion of EphA3-expressing cells using the IIIA4 mAb bound to magnetic beads. Depleted cells were compared to a mock-depleted control.

(B) Orthotopic xenograft experiments were conducted using groups of six NOD/SCID mice injected with 1×10^3, 1×10^4, and 1×10^5 WK1 cells depleted of EphA3 compared to a mock-depleted control. Tumor formation was monitored using in vivo luminescence imaging (Xenogen) over 100 days. Representative images are shown for the 1×10^5 depleted versus control experiment (complete imaging data are shown in Figure S5).

(C) Luminescence imaging of tumor formation was quantitated and showed a significant ($p < 0.05$) reduction in signal between groups. A reduction in tumor formation was observed for all EphA3-depleted groups compared to controls.

(D) Kaplan-Meier survival curves of the 1×10^3 and 1×10^5 cohorts for the WK1 EphA3-depleted cells compared to the mock-depleted control. Depletion of EphA3-expressing cells improved survival compared to the control groups.

(E) qPCR expression analysis of *EPHA3* and the markers *INTEGRIN* α6, *CD133,* and *CD15* in mock- versus EphA3-depleted tumors (+SD, n = 2).

(F) Orthotopic xenograft experiment in NOD/SCID animals using tumor cells from a GBM patient specimen, which had been dissociated and acutely sorted for high versus low EphA3 populations. A total of 5×10^3 tumor cells were injected per animal with six animals per group. The Kaplan-Meier survival curve shows EphA3-positive cells formed tumors with a median survival of 113 days, while no tumor formation was observed in EphA3-low cell-injected animals following 180 days ($p = 0.003$).

(G) A representative coronal H&E section of a tumor formed after injection of EphA3-positive patient tumor cells. Tumors were highly infiltrative and invasive (complete H&E sections for each animal are shown in Figure S5). Scale bar represents 20 μM. See also Figures S5A–S5H.

rescue U251 cells were injected subcutaneously and tumor formation was monitored (Figure S5E). The control tumors (n = 3) reached 1 cm in diameter in an average of 30 days, while the rescue tumors (n = 4) reached 1 cm in diameter in an average of 46 days. The somewhat slower growth of the rescue tumors may reflect the slightly lower EphA3 expression in the rescue cells but confirmed that EphA3 re-expression restored tumorigenic potential.

To confirm that EphA3 is present on tumor cells and not the stromal elements within the tumor, we orthotopically transplanted 5×10^4 tumor cells dissociated directly from a GBM patient specimen into an immune-compromised NOD/SCID animal. Five months following injection, a large invasive tumor was detected. We subsequently analyzed the expression of EphA3 in combination with the human-specific marker major histocompatibility complex class I, human leukocyte antigens (HLA) A, B, and C. Results show a clear separation between nonhuman (mouse) stromal elements that were negative for both EphA3 and HLA-A, B, and C within the tumor and EphA3-positive HLA-A, B, and C tumor cells (Figure 5SF).

To explore whether the observation that EphA3 expression was higher on less differentiated cells and therefore whether low-EphA3 cells might translate into reduced tumorigenicity, we conducted an intracranial EphA3 depletion xenograft experiment using the WK1 primary line infected with a luciferase-encoding lentivirus. Because the EphA3 monoclonal antibody may have activating properties, we initially avoided positive fluorescence-activated cell sorting (FACS) selection and instead compared mock-depleted versus the EphA3 mAb (IIIA4) antibody-depleted cells. As expected, depletion reduced EphA3 levels and also reduced the proliferative and sphere-forming potential of the cells (Figures 5A and S5G). Cohorts of animals were injected intracranially with 1×10^3, 1×10^4, and 1×10^5 cells and tumor formation monitored using in vivo luminescence imaging (Figure 5B; for complete analysis see Figure S5G). Tumor luminescence was quantitated and showed a significant ($p < 0.05$) reduction in signal between mock and control for each injection group (Figure 5C). The protumorigenic effect of EphA3 expression was further confirmed by the survival curves, which showed a significant difference in survival. The median survival for the 1×10^3 group was mock 134 days versus depleted 158 days and for the 1×10^5 group was mock 105 days versus depleted 120 days (Figure 5D). When animals were culled, the tumor was resected and qPCR expression analysis performed for *EPHA3* and markers of less differentiated, highly proliferative cells (Figure 5E). Results showed a minimal

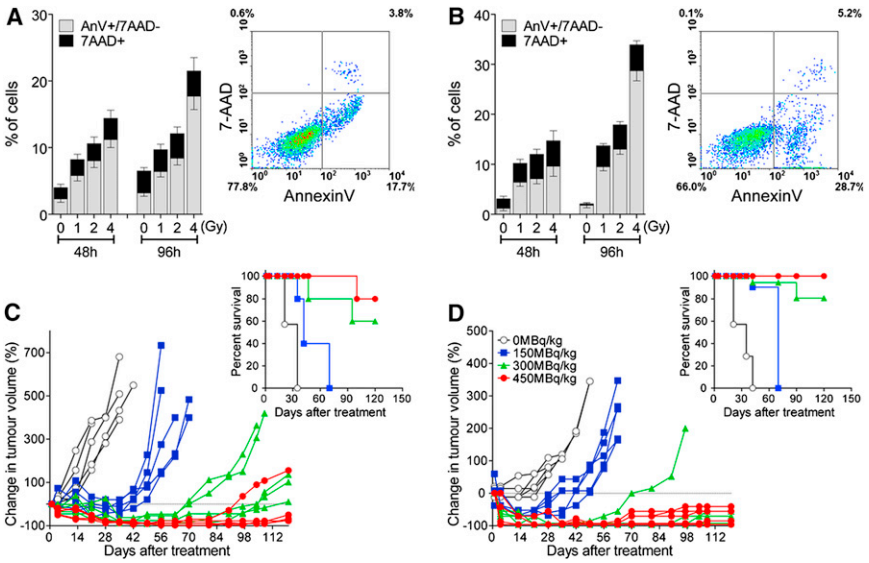

Figure 6. Lutetium-Radiolabelled Anti-EphA3 (IIIA4) mAb Induces Apoptosis and Prevents Tumor Formation

(A and B) U251 (A) and BAH1 (B) cell cultures were treated with unlabeled DOTA-IIIA4 mAb or escalating doses of ^{177}Lu-IIIA4 mAb. At 48 and 96 hr, apoptosis and cell death were analyzed by Annexin V and 7-AAD staining. Representative density plots are shown for the 96 hr time point (inset) after treatment with 4 Gy of ^{177}Lu-IIIA4 mAb. Early apoptotic cells were significantly ($p < 0.01$) higher for all doses and time points compared to cells treated with DOTA-IIIA4 mAb (0 Gy).

(C and D) U251 (C) or BAH1 (D) tumors were grown subcutaneously in BALB/c nude mice (five animals per group). Tumors (50 mm^3) were treated with DOTA-IIIA4 mAb (50 μg per mouse) or escalating doses of ^{177}Lu-IIIA4 mAb (50 μg per mouse). Data are shown as percentage change in tumor volume compared to day 0 (before treatments). Tumor growth curves are shown for individual mice in each treatment group. Insets show Kaplan-Meier survival plots based on tumor volume. One animal bearing a U251 tumor in the 150 MBq/kg showed tumor regrowth and was humanely killed. The survival of 450 MBq/kg ^{177}Lu-IIIA4 mAb-treated mice within the 120-day observation period was 80% and 100% for U251 and BAH-1 xenograft-bearing mice, respectively, whereas the survival after DOTA-IIIA4 mAb (0 MBq/kg) was 0%.

reduction in EphA3 and other markers tested compared to mock-depleted tumors, implying that depleted cells had re-expressed EphA3 by the time the tumors had fully formed.

As a more stringent test of the involvement of EphA3 on the tumor-initiating cell population, a GBM patient tumor was dissociated and acutely sorted for high versus low EphA3 expression. A total of 5 × 10^3 cells from positive and negative fractions were injected orthotopically into NOD/SCID mice (n = 6). The median survival for the positive population was 113 days while no tumors had been detected in the negative fraction at 180 days (Figure 5F). Coronal hematoxylin and eosin (H&E) sections were prepared when animals showed signs of tumor formation. In each case, animals injected with high-EphA3-expressing cells uniformly developed highly infiltrative tumors (Figure 5G; for complete analysis, see Figure S5H). Two animals injected with low-EphA3-expressing tumor cells were culled due to signs of illness, but no tumor formation was detected (Figure S5H).

Radiolabelled Anti-EphA3 mAb Treatment Prevents Tumor Formation

The higher expression of EphA3 on dedifferentiated tumor cells suggested that an EphA3-targeted therapy might extinguish the tumor by eliminating the less differentiated, tumorigenic compartment. To test this idea, we used the EphA3 mAb (IIIA4) radiolabelled with lutetium-177 (^{177}Lu) in mice bearing either U251 or early passage BAH1 cell xenografts. In vitro studies had shown that ^{177}Lu-IIIA4 mAb treatment induced dose- and time-dependent apoptotic cell death in both U251 (Figure 6A) and BAH1 cells (Figure 6B) and reduced clonogenic survival (50% loss of clonogenic survival at 3.5 Gy over 48 hr, data not shown). In mice, following a single injection, the doubling time of U251 tumors was 9.9 ± 0.1 days in DOTA-IIIA4 mAb-treated mice compared to 26.6 ± 0.2 days in mice treated with 150 MBq/kg ^{177}Lu-IIIA4 mAb (Figure 6C). Similarly, in BAH1, 150 MBq/kg ^{177}Lu-IIIA4 mAb lengthened the tumor-doubling time from 12.7 ± 0.1 days in control DOTA-IIIA4 mAb-treated mice to 30.1 ± 1 days (Figure 6D). Higher doses of ^{177}Lu-IIIA4 mAb induced complete regression of both U251 (Figure 6C) and BAH1 (Figure 6D) tumors for up to 9 weeks following treatment. Between 9 and 17 weeks after treatments, regrowth was observed in one out five mice bearing U251 xenografts treated with 450 MBq/kg ^{177}Lu-IIIA4 mAb (Figure 6C) and no regrowth was observed in mice bearing the patient-derived BAH1 xenografts (Figure 6D). Importantly, we observed no weight loss or any clinical signs of toxicity at any of the doses. Kaplan-Meier survival plots (Figures 6C and 6D) based on the defined tumor volume endpoint showed a significant increase in survival upon treatment with ^{177}Lu-IIIA4 mAb ($p < 0.0001$). Given the prolonged follow up after treatment, these results suggest that all tumorigenic cells were effectively targeted by the therapy and at higher doses had extinguished the tumor.

DISCUSSION

The current investigation identifies the EphA3 receptor as being highly expressed on a significant proportion of gliomas and, in particular, on the mesenchymal subtype of GBM. Several lines of evidence show that EphA3 is often more highly expressed on the undifferentiated, tumor-initiating cells. In the first instance, EphA3 was shown to be more highly expressed in serum-free culture systems lacking differentiated cells and was downregulated when cells were differentiated. In tissue sections, the expression of EphA3 was high in areas with few differentiated (GFAP-positive) cells and lower in areas of positive GFAP expression. We observed an association of EphA3 with integrin α6 in patient specimens, a known marker of stem-like cells, but not so clearly with CD133, consistent with heterogeneity within the undifferentiated fraction in GBM (Lathia et al., 2010).

Importantly, we show that EphA3 has a critical role in maintaining GBM cells in an undifferentiated state by limiting MAPK

signaling (model shown in Figure S4E). EphA3 attenuation resulted in partial differentiation and decreased proliferation. Interestingly, if EphA3 was activated sufficiently to induce internalization, then the loss of EphA3 from the cell surface also resulted in reduced cell growth, implying that a relatively small loss of Eph receptor expression results in a shift in the balance between undifferentiated, highly proliferative cells and more differentiated, slowly dividing nontumorigenic cells. Indeed, we show that in lines that coexpress EphA2 or EphA3, loss of either is sufficient to alter this balance toward differentiation. Critically, the presence of EphA3 was shown to be needed for the function of tumor-initiating cells because loss of EphA3 was shown to markedly reduce tumorigenic potential.

Sustained MAPK signaling is able to drive differentiation of neural progenitors (Aoki et al., 2004). Moreover, EphA receptors have been shown to direct differentiation of neural stem cells via the MAPK pathway during CNS development. EphA3 is strongly coexpressed with nestin, a marker of undifferentiated neural cells, in the ventricular zone during murine development and in neurosphere cultures (Aoki et al., 2004). We show that in GBM, loss of EphA3 resulted in elevated MAPK signaling in parallel with partial loss of neurosphere formation, reduced proliferation, and the acquisition of differentiation markers. We show that regulation of ERK/MAPK signaling by EphA3 in GBM is kinase independent and also independent of the upstream activators of MAPK signaling.

The preferential expression of EphA3 in mesenchymal GBM is noteworthy. Mesenchymal tumors behave more aggressively and have a poorer prognosis (Carro et al., 2010; Phillips et al., 2006; Thiery, 2002). Notably, recurrent GBM is associated with a shift to a more mesenchymal state (Phillips et al., 2006). Studies of EphA3 knockout mice show that during heart development, EphA3 expression, induced by EMT, has a critical role in formation of atrioventricular valves and septa (Stephen et al., 2007). These findings suggest that EphA3 expression may increase as part of the switch to a more mesenchymal (sarcomatous) phenotype.

We noted that approximately 40% of GBM clinical specimens expressed significantly increased levels of EphA3 compared to normal brain. A further 20% of specimens expressed lower levels of EphA3 that were still elevated above normal brain tissues. Interestingly, most tumors, when cultured on laminin under conditions preventing differentiation, expressed EphA3 irrespective of subtype. Multiplex flow cytometric analysis of patient specimens revealed a positive association of EphA3 and integrin α6 but not other markers such as CD133. Based on these studies, EphA3 is not restricted to but it is more highly expressed on the less differentiated tumorigenic cells and more widely expressed in less differentiated tumors such as the mesenchymal subtype (Phillips et al., 2006). In some cases, EphA3 appeared to be prominently expressed around the tumor vasculature of GBM xenografts, a known stem cell niche in GBM (Calabrese et al., 2007). A recent study has shown that the laminin receptor integrin α6, a key protein in extracellular matrix modulation, is also localized in the perivascular niche and can regulate tumor-initiating cells (Lathia et al., 2010).

To explore the potential of EphA3 as a therapeutic target, we radiolabelled the EphA3 mAb (IIIA4) using lutetium-177. A single dose of the labeled antibody showed pronounced efficacy in preclinical models with very low toxicity. The failure of tumors to regrow for 16 weeks following ^{177}Lu-IIIA4 mAb treatment strongly suggests that the treatment has targeted the tumor-initiating cell compartment. This supports the development of EphA3-based targeted therapies for the treatment of GBM.

Significantly, we demonstrate that EphA3 plays an active role in maintaining tumor cells in a dedifferentiated, tumorigenic state. Moreover, EphA3 is most highly expressed in the more aggressive and undifferentiated mesenchymal GBM subtype. What then might be the benefits of therapeutic targeting of this cell-surface receptor? EphA3 is expressed at low levels in adult tissues, making it relatively tumor specific. More importantly, our results suggest that such therapy can eliminate the tumor-initiating cells, thereby stopping the tumor at its source.

EXPERIMENTAL PROCEDURES

Patient Tumors

This study was approved by the human ethics committee of the Queensland Institute of Medical Research (QIMR) and Royal Brisbane and Women's Hospital (RBWH). All patients signed an approved consent form prior to surgery. Specimens were examined by a neuropathologist to verify tumor type and grade (Table S1).

GBM Cell Culture

Primary cell lines were derived from GBM specimens and maintained either as primary serum-free cultures grown on laminin (Pollard et al., 2009) or as tumorsphere cultures using StemPro NSC SFM (Invitrogen). The ATCC GBM cell line U251 was cultured in RPMI 1640 media containing 10% FBS or cultured as tumorspheres. All cultures were grown at 37°C under 5% CO_2/95% humidified air.

PCR Analysis

RNA was extracted using TRIzol (Invitrogen). First strand cDNA was synthesized using random hexamers and Superscript III (Invitrogen). Real-time PCR was carried out using SYBR Green (Applied Biosystems). Cycling conditions and primers are listed in Supplemental Experimental Procedures.

shRNA Knock Down

EPHA3 shRNA seq 1 was cloned into pSuperior.neo+gfp (Oligoengine). The inducible KD system was generated using the tetracycline repressor construct pcDNA 6/TR (Invitrogen). *EPHA3* shRNA seq 2 and control construct was the mission lentivirus SCHLNV, Clone ID TRCN0000196830 (Sigma). shRNA sequences are listed in Supplemental Experimental Procedures.

Multiplex Analysis

Two eight-color multiplex analysis was conducted on nine GBM specimens. Cells were selected using a viability dye, hematopoietic lineage cells were excluded using CD45, and CD56 was used to select cells of neural and glial lineage. Cells were analyzed on a LSR 2 (BD); data analysis was carried out using Treestar FlowJo software (version 7.6.4). Antibodies are listed in Supplemental Experimental Procedures.

Amnis Image Stream

Samples were run on an ImageStream^X as previously described (Haney et al., 2011) with minor modification. Briefly, 5,000 events were collected for each sample and single color controls used to create a compensation matrix to correct for spectral overlap. All data were then analyzed using IDEA software (Amnis Corporation, Seattle, WA, USA).

Amnis, IHC, Immunofluorescence, FACS, and Western Blotting Antibodies

For IHC, GFAP (Biocare medical CM065B, 1:1,000), EphA3 in-house mAb (IIIA4, 1:100), and CD31 (Santa Cruz sc1506, 1:100) were used.

For FACS/immunofluorescence, EphA2 in-house mAb (1F7, 5 μg/ml) and EphA3 in-house mAb (IIIA4, 5 μg/ml), CD133 (Miltenyi AC133, 1:10), βIII-tubulin (Promega G712A, 1:100), GFAP (DAKO 20334, 1:100), Integrin α6 (Millipore CBL458, 1:100), myelin basic protein (Sigma M3821, 1:100), and control IgG1 (BD 349040, 1:400) were used.

For western blotting, we used EphA3 in-house rabbit polyclonal (1:2,000), Upstate antibodies ERK1/2 (06-182, 1:1,000), p-ERK1/2 (05-797, 1:1,000), Akt1 (AB3137, 1:1,000), and p-Akt1 (1:1,000), and Stat3 (Santa Cruz 81523, 1:1,000). β-actin was used as a loading control (Sigma, 1:2,000).

Subcutaneous and Orthotopic Xenografts

This study was approved by the QIMR animal ethics committee. Experiments were conducted using 5-week-old NOD/SCID mice. A total of 2×10^6 cells were injected subcutaneously and animals were sacrificed when tumors exceeded 1 cm in diameter. A total of 1×10^5 (for U251 experiments), 1×10^3, 1×10^4, 1×10^5 (for WK1 depletion experiments), and 5×10^3 (for acutely sorted clinical specimen) cells were injected intracranially using a stereotactic device at a depth of 3 mm into the right cerebral hemisphere. Animals were sacrificed when they showed signs of tumor formation (hunching, weight loss, rough coat).

In Vitro and In Vivo Treatment Using ^{177}Lu- IIIA4 mAb

For in vitro studies, ^{177}Lu-IIIA4 mAb (preparation described in Supplemental Experimental Procedures) was diluted to achieve a cumulative dose based on the dose rate constant of ^{177}Lu being 0.283 g.rad/μCi.hr (Kocher, 1981). U251 and BAH1 GBM cultures were subjected to treatments with escalating doses (0–4 Gy) of ^{177}Lu-IIIA4 mAb for 48 or 72 hr and assayed for apoptosis using Annexin V and 7-ADD.

For in vivo studies, BALB/c nude mice were injected subcutaneously with 2×10^6 U251 or BAH1 cells. Treatments with unlabeled DOTA-IIIA4 mAb or escalating doses of ^{177}Lu-labeled DOTA-IIIA4 mAb were initiated when tumors reached 50 mm^3. Unlabeled or labeled IIIA4 mAb was administered intravenously as a single dose. Animals were monitored for clinical signs of toxicity and tumor formation was monitored twice weekly by calliper measurement (detailed in Supplemental Experimental Procedures).

Immunoprecipitation

Serum-starved cultures were lysed in cold lysis buffer and precleared using CnBr inactivated beads. Total protein (2–5mg) was preincubated with either EphA2 (1F7), EphA3 (IIIA4), or EGFR (528) antibodies (1 μg per 1 mg protein) for a minimum of 2 hr at 4°C. Prewashed protein G beads were added with further incubation for 1 hr at 4°C.

Statistical Analysis

A two-tailed Student's t test determined the probability of difference and a p value < 0.05 was considered significant. A χ^2 test was used to evaluate significance of GBM subtypes. Correlation coefficient was determined using parametric linear regression analysis.

SUPPLEMENTAL INFORMATION

Supplemental Information includes one table, five figures, and Supplemental Experimental Procedures and can be found with this article online at http://dx.doi.org/10.1016/j.ccr.2013.01.007.

ACKNOWLEDGMENTS

We thank neurosurgeons Dr. Rosalind Jeffree, Dr. Craig Winter, and Dr. Gert Tolleson from the RBWH, Grace Chojnowski and Paula Hall from the QIMR Flow Cytometry Facility, Dr. Leesa Wockner from the QIMR Statistics Department, Prof. Geoff Hill from the QIMR Bone Marrow Transplant Laboratory, Dr. Trina Yeadon from the QIMR Leukaemia Foundation Research Unit, and Dr. Thomas Robertson from the RBWH Pathology Department. This work was supported by project and program grants from the National Health and Medical Research Council (NHMRC; project grants to A.W.B. and senior principal research fellowship to K.K.K.). This work was supported in part by a grant from Kalabios Pharmaceuticals, Inc.

Received: August 5, 2011
Revised: March 21, 2012
Accepted: January 14, 2013
Published: February 11, 2013

REFERENCES

Aoki, M., Yamashita, T., and Tohyama, M. (2004). EphA receptors direct the differentiation of mammalian neural precursor cells through a mitogen-activated protein kinase-dependent pathway. J. Biol. Chem. *279*, 32643–32650.

Balakrishnan, A., Bleeker, F.E., Lamba, S., Rodolfo, M., Daniotti, M., Scarpa, A., van Tilborg, A.A., Leenstra, S., Zanon, C., and Bardelli, A. (2007). Novel somatic and germline mutations in cancer candidate genes in glioblastoma, melanoma, and pancreatic carcinoma. Cancer Res. *67*, 3545–3550.

Bao, S., Wu, Q., McLendon, R.E., Hao, Y., Shi, Q., Hjelmeland, A.B., Dewhirst, M.W., Bigner, D.D., and Rich, J.N. (2006). Glioma stem cells promote radioresistance by preferential activation of the DNA damage response. Nature *444*, 756–760.

Behin, A., Hoang-Xuan, K., Carpentier, A.F., and Delattre, J.Y. (2003). Primary brain tumours in adults. Lancet *361*, 323–331.

Boyd, A.W., Ward, L.D., Wicks, I.P., Simpson, R.J., Salvaris, E., Wilks, A., Welch, K., Loudovaris, M., Rockman, S., and Busmanis, I. (1992). Isolation and characterization of a novel receptor-type protein tyrosine kinase (*hek*) from a human pre-B cell line. J. Biol. Chem. *267*, 3262–3267.

Calabrese, C., Poppleton, H., Kocak, M., Hogg, T.L., Fuller, C., Hamner, B., Oh, E.Y., Gaber, M.W., Finklestein, D., Allen, M., et al. (2007). A perivascular niche for brain tumor stem cells. Cancer Cell *11*, 69–82.

Carro, M.S., Lim, W.K., Alvarez, M.J., Bollo, R.J., Zhao, X., Snyder, E.Y., Sulman, E.P., Anne, S.L., Doetsch, F., Colman, H., et al. (2010). The transcriptional network for mesenchymal transformation of brain tumours. Nature *463*, 318–325.

Chiari, R., Hames, G., Stroobant, V., Texier, C., Maillère, B., Boon, T., and Coulie, P.G. (2000). Identification of a tumor-specific shared antigen derived from an Eph receptor and presented to CD4 T cells on HLA class II molecules. Cancer Res. *60*, 4855–4863.

Conover, J.C., Doetsch, F., Garcia-Verdugo, J.M., Gale, N.W., Yancopoulos, G.D., and Alvarez-Buylla, A. (2000). Disruption of Eph/ephrin signaling affects migration and proliferation in the adult subventricular zone. Nat. Neurosci. *3*, 1091–1097.

Davies, H., Hunter, C., Smith, R., Stephens, P., Greenman, C., Bignell, G., Teague, J., Butler, A., Edkins, S., Stevens, C., et al. (2005). Somatic mutations of the protein kinase gene family in human lung cancer. Cancer Res. *65*, 7591–7595.

Dick, J.E. (2008). Stem cell concepts renew cancer research. Blood *112*, 4793–4807.

Dottori, M., Down, M., Hüttmann, A., Fitzpatrick, D.R., and Boyd, A.W. (1999). Cloning and characterization of EphA3 (Hek) gene promoter: DNA methylation regulates expression in hematopoietic tumor cells. Blood *94*, 2477–2486.

Flanagan, J.G., and Vanderhaeghen, P. (1998). The ephrins and Eph receptors in neural development. Annu. Rev. Neurosci. *21*, 309–345.

Galli, R., Binda, E., Orfanelli, U., Cipelletti, B., Gritti, A., De Vitis, S., Fiocco, R., Foroni, C., Dimeco, F., and Vescovi, A. (2004). Isolation and characterization of tumorigenic, stem-like neural precursors from human glioblastoma. Cancer Res. *64*, 7011–7021.

Haney, D., Quigley, M.F., Asher, T.E., Ambrozak, D.R., Gostick, E., Price, D.A., Douek, D.C., and Betts, M.R. (2011). Isolation of viable antigen-specific CD8+ T cells based on membrane-bound tumor necrosis factor (TNF)-α expression. J. Immunol. Methods *369*, 33–41.

Holder, N., and Klein, R. (1999). Eph receptors and ephrins: effectors of morphogenesis. Development *126*, 2033–2044.

Holmberg, J., Genander, M., Halford, M.M., Annerén, C., Sondell, M., Chumley, M.J., Silvany, R.E., Henkemeyer, M., and Frisén, J. (2006). EphB receptors coordinate migration and proliferation in the intestinal stem cell niche. Cell *125*, 1151–1163.

Kilpatrick, T.J., Brown, A., Lai, C., Gassmann, M., Goulding, M., and Lemke, G. (1996). Expression of the Tyro4/Mek4/Cek4 gene specifically marks a subset of embryonic motor neurons and their muscle targets. Mol. Cell. Neurosci. *7*, 62–74.

Kocher, D.C. (1981). Radioactive Decay Data Tables: A Handbook of Decay Data for Application to Radiation Dosimetry and Radiological Assessments (Washington, DC: U.S. DOE Technical Information Center; DOE/TIC-11026).

Lathia, J.D., Gallagher, J., Heddleston, J.M., Wang, J., Eyler, C.E., Macswords, J., Wu, Q., Vasanji, A., McLendon, R.E., Hjelmeland, A.B., and Rich, J.N. (2010). Integrin alpha 6 regulates glioblastoma stem cells. Cell Stem Cell *6*, 421–432.

Lawrenson, I.D., Wimmer-Kleikamp, S.H., Lock, P., Schoenwaelder, S.M., Down, M., Boyd, A.W., Alewood, P.F., and Lackmann, M. (2002). Ephrin-A5 induces rounding, blebbing and de-adhesion of EphA3-expressing 293T and melanoma cells by CrkII and Rho-mediated signalling. J. Cell Sci. *115*, 1059–1072.

Li, J.J., Liu, D.P., Liu, G.T., and Xie, D. (2009). EphrinA5 acts as a tumor suppressor in glioma by negative regulation of epidermal growth factor receptor. Oncogene *28*, 1759–1768.

Lickliter, J.D., Smith, F.M., Olsson, J.E., Mackwell, K.L., and Boyd, A.W. (1996). Embryonic stem cells express multiple Eph-subfamily receptor tyrosine kinases. Proc. Natl. Acad. Sci. USA *93*, 145–150.

Lisabeth, E.M., Fernandez, C., and Pasquale, E.B. (2012). Cancer somatic mutations disrupt functions of the EphA3 receptor tyrosine kinase through multiple mechanisms. Biochemistry *51*, 1464–1475.

Mann, F., Peuckert, C., Dehner, F., Zhou, R., and Bolz, J. (2002). Ephrins regulate the formation of terminal axonal arbors during the development of thalamocortical projections. Development *129*, 3945–3955.

Nakada, M., Niska, J.A., Miyamori, H., McDonough, W.S., Wu, J., Sato, H., and Berens, M.E. (2004). The phosphorylation of EphB2 receptor regulates migration and invasion of human glioma cells. Cancer Res. *64*, 3179–3185.

Pardal, R., Clarke, M.F., and Morrison, S.J. (2003). Applying the principles of stem-cell biology to cancer. Nat. Rev. Cancer *3*, 895–902.

Pasquale, E.B. (2010). Eph receptors and ephrins in cancer: bidirectional signalling and beyond. Nat. Rev. Cancer *10*, 165–180.

Phillips, H.S., Kharbanda, S., Chen, R., Forrest, W.F., Soriano, R.H., Wu, T.D., Misra, A., Nigro, J.M., Colman, H., Soroceanu, L., et al. (2006). Molecular subclasses of high-grade glioma predict prognosis, delineate a pattern of disease progression, and resemble stages in neurogenesis. Cancer Cell *9*, 157–173.

Pollard, S.M., Yoshikawa, K., Clarke, I.D., Danovi, D., Stricker, S., Russell, R., Bayani, J., Head, R., Lee, M., Bernstein, M., et al. (2009). Glioma stem cell lines expanded in adherent culture have tumor-specific phenotypes and are suitable for chemical and genetic screens. Cell Stem Cell *4*, 568–580.

Reya, T., Morrison, S.J., Clarke, M.F., and Weissman, I.L. (2001). Stem cells, cancer, and cancer stem cells. Nature *414*, 105–111.

Reynolds, B.A., and Weiss, S. (1992). Generation of neurons and astrocytes from isolated cells of the adult mammalian central nervous system. Science *255*, 1707–1710.

Singh, S.K., Hawkins, C., Clarke, I.D., Squire, J.A., Bayani, J., Hide, T., Henkelman, R.M., Cusimano, M.D., and Dirks, P.B. (2004). Identification of human brain tumour initiating cells. Nature *432*, 396–401.

Son, M.J., Woolard, K., Nam, D.H., Lee, J., and Fine, H.A. (2009). SSEA-1 is an enrichment marker for tumor-initiating cells in human glioblastoma. Cell Stem Cell *4*, 440–452.

Stephen, L.J., Fawkes, A.L., Verhoeve, A., Lemke, G., and Brown, A. (2007). A critical role for the EphA3 receptor tyrosine kinase in heart development. Dev. Biol. *302*, 66–79.

Stupp, R., Mason, W.P., van den Bent, M.J., Weller, M., Fisher, B., Taphoorn, M.J., Belanger, K., Brandes, A.A., Marosi, C., Bogdahn, U., et al.; European Organisation for Research and Treatment of Cancer Brain Tumor and Radiotherapy Groups; National Cancer Institute of Canada Clinical Trials Group. (2005). Radiotherapy plus concomitant and adjuvant temozolomide for glioblastoma. N. Engl. J. Med. *352*, 987–996.

Thiery, J.P. (2002). Epithelial-mesenchymal transitions in tumour progression. Nat. Rev. Cancer *2*, 442–454.

Vearing, C., Lee, F.T., Wimmer-Kleikamp, S., Spirkoska, V., To, C., Stylianou, C., Spanevello, M., Brechbiel, M., Boyd, A.W., Scott, A.M., and Lackmann, M. (2005). Concurrent binding of anti-EphA3 antibody and ephrin-A5 amplifies EphA3 signaling and downstream responses: potential as EphA3-specific tumor-targeting reagents. Cancer Res. *65*, 6745–6754.

Verhaak, R.G., Hoadley, K.A., Purdom, E., Wang, V., Qi, Y., Wilkerson, M.D., Miller, C.R., Ding, L., Golub, T., Mesirov, J.P., et al.; Cancer Genome Atlas Research Network. (2010). Integrated genomic analysis identifies clinically relevant subtypes of glioblastoma characterized by abnormalities in PDGFRA, IDH1, EGFR, and NF1. Cancer Cell *17*, 98–110.

Visvader, J.E. (2011). Cells of origin in cancer. Nature *469*, 314–322.

Wang, L.F., Fokas, E., Juricko, J., You, A., Rose, F., Pagenstecher, A., Engenhart-Cabillic, R., and An, H.X. (2008). Increased expression of EphA7 correlates with adverse outcome in primary and recurrent glioblastoma multiforme patients. BMC Cancer *8*, 79.

Wang, Z., Cohen, K., Shao, Y., Mole, P., Dombkowski, D., and Scadden, D.T. (2004). Ephrin receptor, EphB4, regulates ES cell differentiation of primitive mammalian hemangioblasts, blood, cardiomyocytes, and blood vessels. Blood *103*, 100–109.

Wicks, I.P., Wilkinson, D., Salvaris, E., and Boyd, A.W. (1992). Molecular cloning of HEK, the gene encoding a receptor tyrosine kinase expressed by human lymphoid tumor cell lines. Proc. Natl. Acad. Sci. USA *89*, 1611–1615.

Wilkinson, D.G. (2000). Eph receptors and ephrins: regulators of guidance and assembly. Int. Rev. Cytol. *196*, 177–244.

Wykosky, J., Gibo, D.M., Stanton, C., and Debinski, W. (2005). EphA2 as a novel molecular marker and target in glioblastoma multiforme. Mol. Cancer Res. *3*, 541–551.

Xi, H.Q., Wu, X.S., Wei, B., and Chen, L. (2012). Aberrant expression of EphA3 in gastric carcinoma: correlation with tumor angiogenesis and survival. J. Gastroenterol. *47*, 785–794.